


The Role of Spontaneous Polarization in the Negative Thermal Expansion of Tetragonal PbTiO₃-Based Compounds

Jun Chen,[†] Krishna Nittala,[‡] Jennifer S. Forrester,[‡] Jacob L. Jones,[‡] Jinxia Deng,[†] Ranbo Yu,[†] and Xianran Xing^{*,†,§}

[†]Department of Physical Chemistry and [§]State Key Laboratory for Advanced Metals and Materials, University of Science and Technology Beijing, Beijing 100083, China

[‡]Department of Materials Science and Engineering, University of Florida, Gainesville, Florida 32611-6400, United States

 Supporting Information

ABSTRACT: PbTiO₃-based compounds are well-known ferroelectrics that exhibit a negative thermal expansion more or less in the tetragonal phase. The mechanism of negative thermal expansion has been studied by high-temperature neutron powder diffraction performed on two representative compounds, 0.7PbTiO₃–0.3BiFeO₃ and 0.7PbTiO₃–0.3Bi(Zn_{1/2}Ti_{1/2})O₃, whose negative thermal expansion is contrarily enhanced and weakened, respectively. With increasing temperature up to the Curie temperature, the spontaneous polarization displacement of Pb/Bi ($\delta z_{\text{Pb/Bi}}$) is weakened in 0.7PbTiO₃–0.3BiFeO₃ but well-maintained in 0.7PbTiO₃–0.3Bi(Zn_{1/2}Ti_{1/2})O₃. There is an apparent correlation between tetragonality (c/a) and spontaneous polarization. Direct experimental evidence indicates that the spontaneous polarization originating from Pb/Bi–O hybridization is strongly associated with the negative thermal expansion. This mechanism can be used as a guide for the future design of negative thermal expansion of phase-transforming oxides.

It is well-known that thermal expansion is a phenomenon for instance due to the inherent anharmonicity of bond vibrations. However, negative thermal expansion (NTE) over a certain temperature range has been found for some materials, including oxides, alloys, and so on.^{1–11} The discovery of NTE immediately enabled possible routes for reducing the problems of thermal expansion in various applications.² To date, the nature of well-studied NTE materials has been more correlated with the effect of thermal vibrations of the framework materials, such as the coupled rigid polyhedra in ZrW₂O₈^{1,2} and the geometric flexibility of metal–cyanide–metal linkages in Ag₃[Co(CN)₆].³ However, NTE in a considerable number of structures is convoluted with nonvibrational effects such as contributions from bonding and electrons.^{2c,5–8} Generally, the NTE is coupled with physical properties, such as the magnetic transition for Invar alloys and nanoparticles of CuO and Au^{5–7} and the change of valence state in the transition-metal oxide LaCu₃Fe₄O₁₂.⁸ A well-developed understanding of the origin of NTE in different types of materials shows promise to enable even more applications.

PbTiO₃ (PT) is a prototype ferroelectric with a spontaneous polarization (P_S) parallel to the polar direction of the c axis. Compounds related to PT-based perovskites have been widely used in the last half century in the fields of dielectrics, piezoelectrics,

ferroelectricities, and so on.¹² Besides the above well-known electronic properties, almost all tetragonal PT-based compounds unconventionally exhibit NTE, which is rarely observed in other perovskites.¹¹ Furthermore, through the use of desirable substitutions for Pb or Ti cations, the coefficient of thermal expansion (CTE) of PT can be widely controlled, almost covering the range of CTEs previously reported for NTE oxides. Not only large NTE but also nearly zero thermal expansion (ZTE) can be realized over a wide temperature range. For example, the NTE was enhanced in $(1-x)\text{PbTiO}_3-x\text{BiFeO}_3$ (CTE = $-3.92 \times 10^{-5} \text{ }^\circ\text{C}^{-1}$ for $x = 0.6$)^{11c} and $(\text{Pb}_{1-x}\text{Cd}_x)\text{TiO}_3$ (CTE = $-2.40 \times 10^{-5} \text{ }^\circ\text{C}^{-1}$ for $x = 0.06$),^{11d} while near ZTE was achieved in $(1-x)\text{PbTiO}_3-x\text{Bi}(\text{Zn}_{1/2}\text{Ti}_{1/2})\text{O}_3$ (CTE = $-0.60 \times 10^{-5} \text{ }^\circ\text{C}^{-1}$ for $x = 0.3$)^{11a} and $(1-x)\text{PbTiO}_3-x\text{Bi}(\text{Ni}_{1/2}\text{Ti}_{1/2})\text{O}_3$ (CTE = $0.12 \times 10^{-5} \text{ }^\circ\text{C}^{-1}$ for $x = 0.2$).^{11b} Since significantly different NTE behaviors exist in PT-based perovskites, an understanding of the mechanism of such behavior may prove to be a useful tool in controlling NTE. It was expected that the tetragonality (c/a) could indicate NTE, since c/a is correlated with the lattice distortion; however, several exceptions where ZTE unexpectedly coexists with large c/a have been found.^{11a} Therefore, an illumination of the NTE mechanism will help us consciously control NTE and tailor thermal expansion. The NTE mechanism was primarily understood according to our previous lattice dynamics studies of the $A_1(1\text{TO})$ soft mode representing the opposite vibration along the spontaneous polarization direction.^{11a} However, no direct evidence for the mechanism of NTE was found. In the present work, the temperature dependence of the structure was investigated by means of high-temperature neutron powder diffraction (NPD) of two representative PT-based compounds, 0.7PbTiO₃–0.3BiFeO₃ (PT–BF30) and 0.7PT–0.3Bi(Zn_{1/2}Ti_{1/2})O₃ (PT–BZT30), which show enhanced NTE and ZTE, respectively. A strong experimental correlation between the spontaneous polarization and NTE was found for the PT-based ferroelectrics, which are important branch of the NTE family.

The samples of PT–BF30 and PT–BZT30 were prepared by a solid-state reaction using simple oxides (PbO, Bi₂O₃, ZnO, Fe₂O₃, and TiO₂) as precursors. Sample preparation details are given in the Supporting Information (SI). High-temperature NPD data were collected over an angular range of 10–130° at a wavelength of 1.5359 Å on the Neutron Powder Diffractometer (HB-2A) at the High Flux Isotope Reactor at Oak Ridge National

Received: May 20, 2011

Published: June 22, 2011

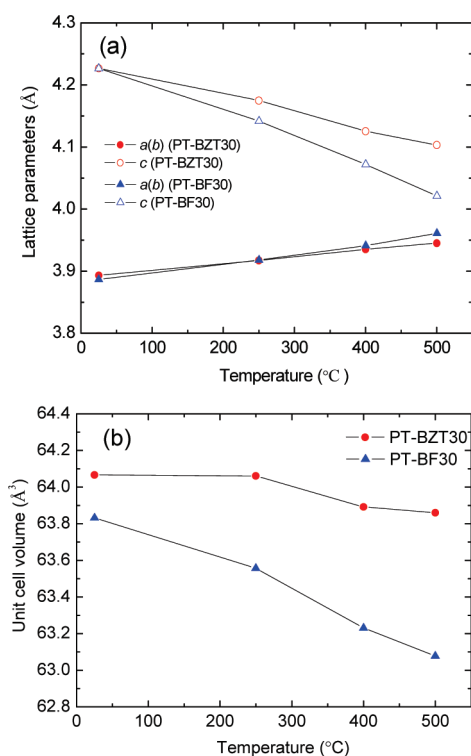


Figure 1. (a) Lattice parameters [$a(b)$ axis and c axis] and (b) unit cell volume of $0.7\text{PbTiO}_3-0.3\text{Bi}(\text{Zn}_{1/2}\text{Ti}_{1/2})\text{O}_3$ (PT-BZT30) and $0.7\text{PbTiO}_3-0.3\text{BiFeO}_3$ (PT-BF30) as functions of temperature.

Laboratory. The structure was refined using FULLPROF Rietveld refinement software by adopting the same initial model ($P4mm$, No. 99) as for PT.^{13,14}

PT-BF30 and PT-BZT30 belong to the perovskite-type $\text{PbTiO}_3-\text{BiMO}_3$ [where M represents cation(s) with an average valence of +3] family of materials, which were recently developed as high Curie temperature (T_C) and high-performance Bi-based piezoelectrics.^{15–21} It is interesting to find some unexpected structural properties due to the special strong hybridization of $\text{Bi}(6s)-\text{O}(2p)$ bonding and coupling between A-site and B-site cations with strong ferroelectric activity.^{16,17} For example, c/a and T_C are abnormally enhanced in several systems ($M = \text{Fe}, \text{Zn}_{1/2}\text{Ti}_{1/2}, \text{Zn}_{1/2}\text{Zr}_{1/2}$).^{16,18,19} T_C has also been shown to be nonmonotonic with respect to the content of BiMO_3 ($M = \text{Sc}, \text{Mg}_{1/2}\text{Ti}_{1/2}$).^{16,18,21} Moreover, their CTE behavior scatters dramatically, and the NTE mechanism is unclear because of the strong dependence on composition.¹¹ Among PT-based compounds, PT-BF30 and PT-BZT30 exhibit similar enhanced c/a and T_C values (PT-BF30, $c/a = 1.091$ and $T_C = 565$ °C; PT-BZT30, $c/a = 1.092$ and $T_C = 650$ °C).^{18,19} However, their NTEs behave oppositely, being much enhanced in PT-BF30 ($\text{CTE} = -2.38 \times 10^{-5} \text{ }^\circ\text{C}^{-1}$) and weakened in PT-BZT30 ($\text{CTE} = -0.60 \times 10^{-5} \text{ }^\circ\text{C}^{-1}$).^{11a,c} Such a pronounced difference in the NTE provides an opportunity to reveal the NTE mechanism. The temperature dependence of the structures of PT-BF30 and PT-BZT30 was therefore studied by means of NPD.

The temperature dependence of the lattice parameters of PT-BF30 and PT-BZT30 is shown in Figure 1a. These results demonstrate that temperature strongly affects the c axis of PT-BZT30 and PT-BF30, more dramatically affecting the latter. In contrast, the $a(b)$ lattice parameters increase but to a

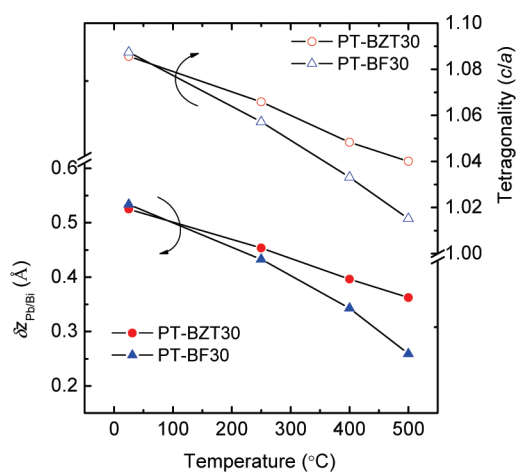


Figure 2. Tetragonality (c/a) and P_S displacement of Pb/Bi ($\delta z_{\text{Pb/Bi}}$) in PT-BZT30 and PT-BF30 as functions of temperature.

smaller extent. Therefore, the unit cell volume (a^2c) is dominated by the c axis, which is also a common character for PT-based compounds.^{11a} According to the first-principles and experimental results, the relatively small temperature dependence of the $a(b)$ lattice parameters is related to the fact that the B-site Ti cation is more strongly covalent with the four neighboring oxygens O2 in the ab plane than with the two O1 oxygens (O1–Ti–O1) along the c axis. The stiff Ti–O2 bonds make compression and elongation in the ab plane energetically unfavorable, while the bonds of the O1–Ti–O1 unit along the c axis (i.e., the polar direction) are soft.^{22,23} As shown in Figure 1b, a low NTE in PT-BZT30 and an enhanced NTE in PT-BF30 are produced. It should be noted that the ceramic sintering process is much influenced by their discrepant NTEs: PT-BZT30 ceramics have better sintering characteristics because of the low thermal expansion, whereas it is too difficult to sinter dense PT-BF30 ceramics because of the strong NTE.

Since the trend of the unit cell volume is considerably controlled by the evolution of the c axis as a function of temperature, we used the tetragonality (c/a) to trace the NTE. Figure 2 depicts the temperature dependence of c/a for the two materials. The c/a values are similar at room temperature (RT) but gradually separate from one another with increasing temperature. The larger decrease of c/a for PT-BF30 results in enhanced NTE, which can be demonstrated by comparison of Figures 1b and 2.

It is well-known that lattice distortion can be described by the tolerance factor t , which is defined as

$$t = \frac{R_A + R_O}{\sqrt{2}(R_B + R_O)}$$

where R_A , R_B , and R_O are the radii for the A, B, and oxygen atoms, respectively. The values of t for PT-BF30 ($t = 0.9974$) and PT-BZT30 ($t = 0.9933$) are very close. This could reasonably account for their similar c/a values at RT. However, it fails to explain the big difference in their c/a values at high temperatures, such as 500 °C. What is the mechanism of NTE in the PT? It is known that the large ferroelectric polarization of PT originates from the unique strong hybridization of the Pb 6s and O 2p orbitals, resulting in the large lattice strain. Such an A–O interaction is weak or ionic in other non-Pb compounds, such as BaTiO_3 .²² It is interesting to note that the

NTE is a common property of tetragonal Pb-based compounds but not of other non-Pb compounds. We believe that there is a strong coupling between the spontaneous polarization and the NTE, which was preliminarily suggested by the lattice dynamics results.^{11a}

Here the spontaneous polarization displacement of Pb/Bi ($\delta z_{\text{Pb/Bi}}$) was derived from the NPD refinement. $\delta z_{\text{Pb/Bi}}$ is defined as the distance from the Pb/Bi atom to the centroid of the oxygen polyhedron. The refined values of $\delta z_{\text{Pb/Bi}}$ as a function of temperature are also shown in Figure 2. At RT, the $\delta z_{\text{Pb/Bi}}$ values for PT-BF30 (0.534 Å) and PT-BZT30 (0.525 Å) are larger than that of pure PT (0.468 Å),¹³ suggesting enhanced ferroelectricity due to the strong Pb/Bi–O hybridization and coupling interactions from the B-site Fe, Ti, and Zn cations with high ferroelectric activity.¹⁷ However, with increasing temperature, $\delta z_{\text{Pb/Bi}}$ is influenced much differently by temperature. It drops more rapidly for PT-BF30, which suggests that the Pb/Bi–O hybridization is more weakened relative to that in PT-BZT30. This reinforces the observation that the temperature evolution of $\delta z_{\text{Pb/Bi}}$ scales linearly with the previously reported Raman-active $A_1(1\text{TO})$ mode, which represents the opposite vibration along the polarization direction for both PT-BF30 and PT-BZT30 (Figure S7 in the SI).²⁴ Furthermore, the temperature-dependent polarization can be also indicated by the variation of the four short Pb–O2 bonds, since the Pb atom forms covalent bonds only with the four nearest-neighbor oxygens.²³ The Pb–O2 bonds elongate more quickly as function of temperature for PT-BF30 (Figure S8), demonstrating the more weakened Pb/Bi–O interaction and thus more decreased $\delta z_{\text{Pb/Bi}}$.

As shown in Figure 2, it is apparent that there is a strong coupling interaction between c/a and $\delta z_{\text{Pb/Bi}}$ (i.e., between the NTE and spontaneous polarization). With increasing temperature up to T_C , $\delta z_{\text{Pb/Bi}}$ decreases more rapidly for PT-BF30, resulting in relaxation of the lattice strain and the strong NTE. However, PT-BZT30 maintains the spontaneous polarization, which produces a low thermal expansion.

Figure 3a shows the correlation between $c/a - 1$ and $\delta z_{\text{Pb/Bi}}^2$ for PT-BF30 and PT-BZT30. There is a strongly linear relationship between $c/a - 1$ and $\delta z_{\text{Pb/Bi}}^2$ that is distributed along the straight line crossing to the coordinate origin. This relationship is similar to the Landau theory relationship $T_C = \alpha P_S^2$.^{16,21,25} With increasing temperature, PT-BF30 moves closer than PT-BZT30 to the origin along the fitted straight line. The proximity to the origin means more weakened spontaneous polarization and thus more enhanced NTE. The NTE of PT has a strong correlation to the spontaneous polarization (Figure 3b).

The trend in Figure 3a can guide the design and control of the NTE. For enhanced NTE, the spontaneous polarization should change with temperature on a scale that is as large as possible. A low thermal expansion could be achieved by decreasing the range of spontaneous polarization variation as function of temperature.

High-temperature NPD has been carried out to investigate the structures of two representative compounds, PT-BF30 and PT-BZT30, which show enhanced NTE and low thermal expansion, respectively. The temperature dependence of c/a is strongly coupled with the spontaneous polarization displacement of Pb/Bi. Direct experimental evidence that the spontaneous polarization is strongly correlated to the NTE of PT-based compounds has been found. The design of NTE in future studies has also been suggested.

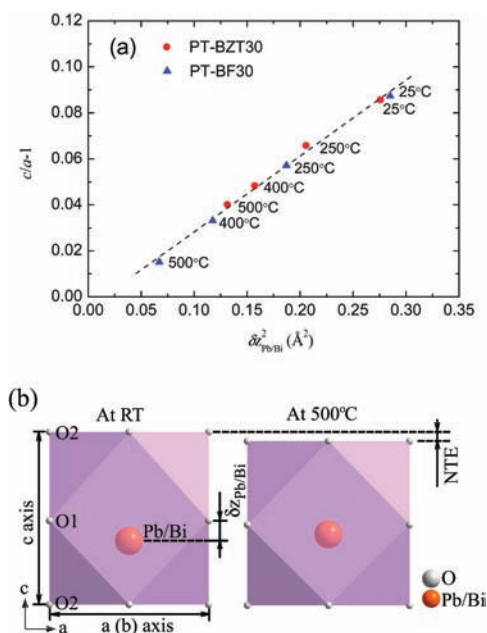


Figure 3. (a) Linear correlation between $c/a - 1$ and $\delta z_{\text{Pb/Bi}}^2$ for PT-BZT30 and PT-BF30 over the temperature range from RT to 500 °C. (b) Schematic illustration of the role of spontaneous polarization ($\delta z_{\text{Pb/Bi}}$) in NTE. The PbO₁₂ polyhedron is projected along the b-axis direction.

ASSOCIATED CONTENT

S Supporting Information. Neutron powder diffraction patterns, structure, and Raman soft mode. This material is available free of charge via the Internet at <http://pubs.acs.org>.

AUTHOR INFORMATION

Corresponding Author
xing@ustb.edu.cn

ACKNOWLEDGMENT

This work was supported by the National Natural Science Foundation of China (Grants 91022016, 21031005, 50725415, and 20731001) and the Fundamental Research Funds for the Central Universities, China (Grant FRF-TP-09-004B). J.L.J. and J.S.F. acknowledge support from the U.S. Department of the Army under W911NF-09-1-0435. The NPD measurements performed at Oak Ridge National Laboratory's High Flux Isotope Reactor were sponsored by the Scientific User Facilities Division, Office of Basic Energy Sciences, U.S. Department of Energy, under Proposal 3095. The assistance of Dr. Clarina de la Cruz and Dr. Ovidiu Garlea at the Neutron Powder Diffractometer (HB-2A) is greatly appreciated.

REFERENCES

- Mary, T. A.; Evans, J. S. O.; Vogt, T.; Sleight, A. W. *Science* **1996**, *272*, 90–92.
- (a) Sleight, A. W. *Inorg. Chem.* **1998**, *37*, 2854–2860. (b) Evans, J. S. O. *J. Chem. Soc., Dalton Trans.* **1999**, 3317–3326. (c) Barrera, G. D.; Bruno, J. A. O.; Barron, T. H. K.; Allan, N. L. *J. Phys.: Condens. Matter* **2005**, *17*, R217–R252.
- Goodwin, A. L.; Calleja, M.; Conterio, M. J.; Dove, M. T.; Evans, J. S. O.; Keen, D. A.; Peters, L.; Tucker, M. G. *Science* **2008**, *319*, 794–797.

- (4) Margadonna, S.; Prassides, K.; Fitch, A. N. *J. Am. Chem. Soc.* **2004**, *126*, 15390–15391.
- (5) Mohn, P. *Nature* **1999**, *400*, 18–19.
- (6) Zheng, X. G.; Kubozono, H.; Yamada, H.; Kato, K.; Ishiwata, Y.; Xu, C. N. *Nat. Nanotechnol.* **2008**, *3*, 724–726.
- (7) Li, W.-H.; Wu, S. Y.; Yang, C. C.; Lai, S. K.; Lee, K. C. *Phys. Rev. Lett.* **2002**, *89*, No. 135504.
- (8) Long, Y. W.; Hayashi, N.; Saito, T.; Azuma, M.; Muranaka, S.; Shimakawa, Y. *Nature* **2009**, *458*, 60–63.
- (9) Roy, R.; Agrawal, D. K.; McKinsty, H. A. *Annu. Rev. Mater. Sci.* **1989**, *19*, 59–81.
- (10) Kwon, Y.-K.; Berber, S.; Tománek, D. *Phys. Rev. Lett.* **2004**, *92* No. 015901.
- (11) (a) Chen, J.; Xing, X. R.; Sun, C.; Hu, P.; Yu, R. B.; Wang, X. W.; Li, L. H. *J. Am. Chem. Soc.* **2008**, *130*, 1144–1145. (b) Hu, P.; Chen, J.; Deng, J. X.; Xing, X. R. *J. Am. Chem. Soc.* **2010**, *132*, 1925–1928. (c) Chen, J.; Xing, X. R.; Liu, G. R.; Li, J. H.; Liu, Y. T. *Appl. Phys. Lett.* **2006**, *89*, No. 101914. (d) Chen, J.; Xing, X. R.; Yu, R. B.; Liu, G. R. *Appl. Phys. Lett.* **2005**, *87*, No. 231915.
- (12) Haertling, G. H. *J. Am. Ceram. Soc.* **1999**, *82*, 797–818.
- (13) Shirane, G.; Pepinsky, R.; Frazer, B. C. *Acta Crystallogr.* **1956**, *9*, 131–140.
- (14) Roisnel, T.; Rodriguez-Carvajal, J. *Mater. Sci. Forum* **2001**, *378–381*, 118–123.
- (15) Eitel, R. E.; Randall, C. A.; Shrout, T. R.; Rehrig, P. W.; Hackenberger, W.; Park, S.-E. *Jpn. J. Appl. Phys.* **2001**, *40*, S999–6002.
- (16) Grinberg, I.; Rappe, A. M. *Phys. Rev. Lett.* **2007**, *98*, No. 037603.
- (17) Grinberg, I.; Suchomel, M. R.; Davies, P. K.; Rappe, A. M. *J. Appl. Phys.* **2005**, *98*, No. 094111.
- (18) Stringer, C. J.; Shrout, T. R.; Randall, C. A.; Reaney, I. M. *J. Appl. Phys.* **2006**, *99*, No. 024106.
- (19) Suchomel, M. R.; Davies, P. K. *Appl. Phys. Lett.* **2005**, *86*, No. 262905.
- (20) Grinberg, I.; Suchomel, M. R.; Dmowski, W.; Mason, S. E.; Wu, H.; Davies, P. K.; Rappe, A. M. *Phys. Rev. Lett.* **2007**, *98*, No. 107601.
- (21) Chen, J.; Nittala, K.; Jones, J. L.; Hu, P.; Xing, X. R. *Appl. Phys. Lett.* **2010**, *96*, No. 252908.
- (22) Cohen, R. E. *Nature* **1992**, *358*, 136–138.
- (23) Kuroiwa, Y.; Aoyagi, S.; Sawada, A.; Harada, J.; Nishibori, E.; Takata, M.; Sakata, M. *Phys. Rev. Lett.* **2001**, *87*, No. 217601.
- (24) (a) Burns, G.; Scott, B. A. *Phys. Rev. B* **1973**, *7*, 3088–3101. (b) Foster, C. M.; Grimsditch, M.; Li, Z.; Karpov, V. G. *Phys. Rev. Lett.* **1993**, *71*, 1258–1260.
- (25) Abrahams, S. C.; Kurtz, S. K.; Jamieson, P. B. *Phys. Rev.* **1968**, *172*, 551–553.